Bioorganic Chemistry 40 (2012) 92–98

Contents lists available at SciVerse ScienceDirect

Bioorganic Chemistry

journal homepage: www.elsevier.com/locate/bioorg

Modifications of ribonuclease A induced by *p*-benzoquinone

Jisook Kim [a,*], Albert R. Vaughn [a], Chris Cho [a], Titus V. Albu [b], Ethan A. Carver [c]

[a] Department of Chemistry, Box 2252, University of Tennessee at Chattanooga, Chattanooga, TN 37403, United States
[b] Department of Chemistry, Box 5055, Tennessee Technological University, Cookeville, TN 38505, United States
[c] Department of Biological and Environmental Sciences, Box 2653, University of Tennessee at Chattanooga, Chattanooga, TN 37403, United States

ARTICLE INFO

Article history:
Received 21 August 2011
Available online 19 November 2011

Keywords:
Benzoquinone
PAH quinones
Ribonuclease A
Protein aggregation

ABSTRACT

The nature of ribonuclease A (RNase) modifications induced by *p*-benzoquinone (pBQ) was investigated using several analysis methods. SDS–PAGE experiments revealed that pBQ was efficient in producing oligomers and polymeric aggregates when RNase was incubated with pBQ. The fluorescence behavior and anisotropy changes of the modified RNase were monitored for a series of incubation reactions where RNase (0.050 mM) was incubated with pBQ (0.050, 0.25, 0.50, 1.50 mM) at 37 °C in phosphate buffer (pH 7.0, 50 mM). The modified RNase exhibited less intense fluorescence and slightly higher anisotropy than the unmodified RNase. UV–Vis spectroscopy indicated that pBQ formed covalent bonds to the modified RNase. Confocal imaging analysis confirmed the formation of the polymeric RNase aggregates with different sizes upon exposure of RNase to high concentrations of pBQ. The interaction between the modified RNase and salts affecting biomineralization of salts was also investigated by scanning electron microscopy. Overall, our results show that pBQ can induce formation of both RNase adducts and aggregates thus providing a better understanding of its biological activity.

1. Introduction

p-Benzoquinone (pBQ) belongs to the family of polycyclic aromatic hydrocarbon (PAH) quinones and is known to be linked with leukemogenesis generated by benzene [1–4]. It has been thought that PAH quinones such as pBQ exhibit their toxicity by reacting with cellular proteins and nucleic acids mainly through redox cycling [5,6] and adduct formation (Fig. 1) [3,4,7–22]. Published studies have focused heavily on the adduct formation of pBQ and biomolecules [3,4,7–22]. Among these studies, Lau and coworkers' findings provide a thorough insight on the complex nature of pBQ-induced adduct formation that can involve either a cyclized diquinone-lysine adduct or a Michael adduct of pBQ and glutamic acid [18–21]. Krajewska and coworkers found that arylation of thiol groups as well as oxidations of thiols are responsible for the inhibition of urease by a series of quinones [22]. In addition to the cases focused on redox cycling and adduct formation, one can postulate another pathway where pBQ induces protein cross-linking which can alter the integrity of proteins, thus contributing to toxicity. As shown in the model scheme in Fig. 1, pBQ can react with a nucleophilic lysine residue of a protein resulting in lysine oxidation, which can lead to the formation of allysine (*i.e.*, aldehyde containing lysine) [23]. The allysine can then condense with an intact lysine residue from another protein molecule generating intramolecular cross-linking. Repeated cross-linking may ultimately cause the formation of oligomers and furthermore polymeric aggregates.

Protein aggregation, whether guided or self-assembled, is a commonly occurring event in biological systems. In recent years, interest on protein aggregation increased due to mounting evidence illustrating a close correlation between protein aggregation and disorders such as Parkinson's disease, Alzheimer's disease, and Huntington's disease [24–29]. Such aggregation was explored with a wide range of proteins such as lysozyme [30,31], ovalbumin [32], huntingtin exon [33], and human serum albumin [34,35], under various conditions. As to how protein aggregation occurs, a lot of details remain to be investigated. One obvious consensus is that destabilized proteins may undergo aggregation in an effort to minimize the free energy of the destabilized conformation as pointed out by Gregersen and Dobson's independent studies [25,27,29]. It is also understood that proteins' physicochemical properties and their interaction with the surrounding environment, such as pH [35,36], pressure [37], temperature [33,38], mutation [31], and the presence of destabilizing chemicals [32–36], contribute to the degree of aggregation. Among these aggregation factors, our laboratory has been interested in the role of destabilizing chemicals, in particular pBQ, a PAH quinone. PAH quinone-induced protein aggregation has received very little attention. Considering the expected ability of PAH quinones to generate protein cross-linking leading to aggregation, investigating the nature of protein modifications induced by

Abbreviations: RNase, ribonuclease A; pBQ, *p*-benzoquinone; HQ, hydroquinone; MW, molecular weight; A_x, absorbance at *x* nm; TCA, trichloroacetic acid.

* Corresponding author. Fax: +1 423 425 5234.
E-mail address: jisook-kim@utc.edu (J. Kim).

0045-2068/$ - see front matter © 2011 Elsevier Inc. All rights reserved.
doi:10.1016/j.bioorg.2011.11.002

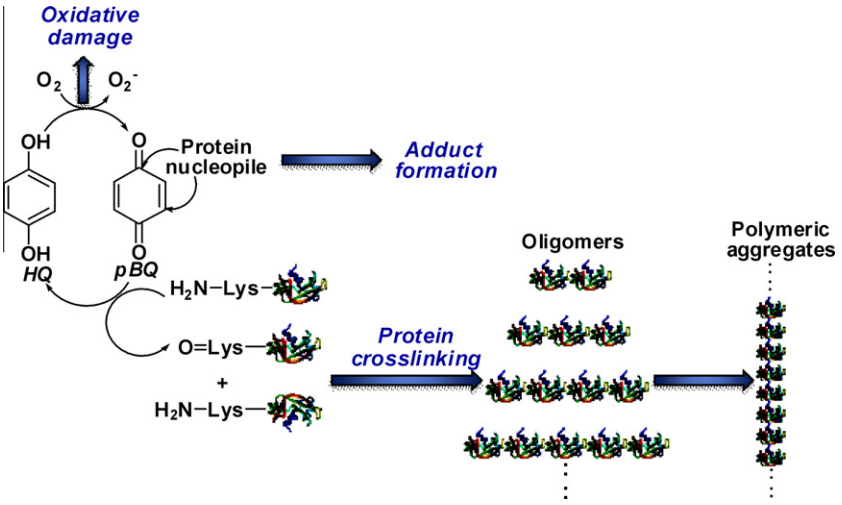

Fig. 1. Proposed mechanism of pBQ action.

pBQ including aggregation will offer a thorough understanding on how PAH quinones exhibit toxicity.

In this context, we report here the results of a study on the modification nature of a target protein, ribonuclease A (RNase), upon exposure to pBQ. We used a variety of methods including SDS–PAGE, fluorescence spectroscopy, UV–Vis spectroscopy, confocal microscopy, and scanning electron microscopy. RNase was chosen for this study because it is relatively stable, and it has been used in several studies of protein modification [16,17,39–41]. SDS–PAGE was utilized to observe changes in the molecular weight (MW) of RNase in the presence of pBQ. To explore the structural and morphological changes of RNase, fluorescence spectroscopic measurements were coupled with UV–Vis spectroscopy and confocal microscopy. In addition to these characterizations, we also investigated the effect of the modified RNase on biomineralization. Recently, interest on biomineralization increased in an effort to understand the interaction between salts and proteins in biological systems [32,42]. The work of Talapatra and coworkers clearly shows that there is a strong connection between the fibrillation of egg white ovalbumin and biomineralization of NaCl and KCl [32]. On the other hand, Tremel and coworkers found that the presence of minerals resulted in protein unfolding [42]. Hence, the purpose of our investigation was to offer valuable insight into protein modifications induced by pBQ by examining not only the physical behavior of the modified RNase but also the interaction with the surrounding salt environments.

2. Materials and methods

All chemicals were purchased from Fisher and of reagent grade unless specified otherwise. The water used in the study was deionized water (dI-water) purified by a Millipore system (Milli-Q water). Ribonuclease A (from *bovine pancreas*) was purchased from Sigma (Cat. # R6513-250MG). Electrophoresis units for minigels were purchased from Fisher. Dialysis was carried out using a 3-mL Float-A-Lyzer with a molecular weight cutoff of 3.5 kDa, which was purchased from Spectrum Laboratories.

2.1. RNase modification detected by 1D SDS–PAGE

Aliquots of an RNase stock solution were diluted to have a final concentration of 0.145 mM and were reacted with pBQ at 0.50 and 5.0 mM in phosphate buffer (pH 7.0, 50 mM). Then, an aliquot of the reaction mixture was taken out at various time periods, followed by immediate cooling at 0 °C. To the samples containing RNase, cold trichloroacetic acid (TCA) on ice was added to have a final concentration of TCA at 20%. The mixture was left on ice for 10 min for precipitation. The sample was then centrifuged at 12,000 rpm for 20 min at 4 °C. The supernatant was decanted and submitted to the further analysis as needed. The pellet was rinsed twice with an ice-cold washing solution. The washed pellet was reconstituted in tris buffer (25 mM tris, 192 mM glycine, 0.10% SDS at pH 8.3). The aliquot (20 μL) of the reconstituted pellet fractions was submitted to the electrophoretic analysis as described below.

For the SDS–PAGE analysis, all proteins were separated on a 10% SDS–PAGE gel according to the method of Laemmli [43]. Pierce Blue Prestained Protein Molecular Weight Marker Mix (Cat. # 26681) was used as a reference for gel electrophoresis experiments as needed. There are seven proteins in the molecular marker: myosin, 215 kDa; phosphorylase B, 120 kDa; BSA, 84 kDa; ovalbumin, 60 kDa; carbonic anhydrase, 39.2 kDa; trypsin inhibitor, 28 kDa; and lysozyme, 18.3 kDa. Prior to loading, samples were mixed with equal volume of SDS–PAGE electrophoresis loading buffer (250 mM tris, pH 6.8; 10% SDS; 10 mM 2-mercaptoethanol; 20% glycerol; 0.015% bromophenol blue) and then the residue was heated at 100 °C for 5 min. Electrophoresis was performed for 2.5 h at 100 V and 60 mA for two gels (30 mA per gel). Protein bands were visualized by staining the gels with 0.1% coomassie brilliant blue R-250 blue dissolved in methanol:acetic acid:dI-water (2.5:1:6.5 by volume) prior to destaining in methanol:acetic acid:dI-water (2.5:1:6.5 by volume). Molecular weight (MW) of each protein band was determined by plotting the mobility represented in the distance each band traveled against the logarithm of the protein MW using the Protein Molecular Weight Marker [44].

2.2. RNase modification detected by fluorescence spectroscopy

Fluorescence spectra and anisotropy values were obtained at 37 °C using a Horiba Jobin Yvon Fluorolog-3 spectrophotometer with polarization accessories and a full-spectrum xenon lamp. The samples were recorded in a 1 cm × 1 cm quartz cuvette using an excitation wavelength of 280 nm. All emission spectra were recorded over the 290–550 nm range in increments of 1 nm, with a band pass of 2 nm for both excitation and emission, and were corrected for the lamp, the monochromators, and the detector response. The spectrum of the unmodified RNase was recorded with an integration time of 0.5 s, while the spectra of the modified

(*i.e.*, post-dialysis) RNase and RNase-pBQ reaction mixtures were recorded with an integration time of 0.1 s. The spectra of the unmodified and the post-dialysis RNase were normalized in the 365–400 nm range, where the tyrosine emission is negligible. The steady-state anisotropy values were determined with a band pass of 5 nm for both excitation and emission and with an integration time of 5 s.

All fluorescence studies were carried out in a phosphate buffer (pH 7.0, 50 mM) solution. The concentration of RNase in the reaction mixture was always 0.050 mM and was obtained by transferring aliquots of an RNase stock solution. pBQ concentrations were 0.050, 0.25, 0.50, and 1.50 mM, respectively, and were obtained from fresh pBQ stock solutions that were prepared each time and used immediately after sonication for 10 min. The reaction was initiated by adding the appropriate volume (always less than 100 μL) of pBQ stock solution to a solution containing RNase that was equilibrated at 37 °C in the temperature-controlled cell holder of the fluorometer for 15 min. The RNase modifications were monitored every 1 h for 24 h. Following the fluorescence monitoring, the reaction mixture was dialyzed against phosphate buffer (pH 7.0, 50 mM) at 4 °C for 24 h. The dialyzed samples, which will be called further as the modified RNase or the post-dialysis RNase, were submitted to additional analysis as presented below. Control RNase was subjected to the same procedure except the addition of pBQ.

2.3. UV–Vis analysis of the modified RNase

The UV–Vis spectra of the modified RNase were obtained using a Shimadzu Biospec-1601 spectrophotometer equipped with the temperature-controlled cell holder which was equilibrated at 37 °C. Software used for data collection was UV Probe 2.3 by Shimadzu. The unmodified RNase and the post-dialysis RNase samples were recorded in a 1 cm × 1 cm quartz cuvette.

2.4. Confocal microscopy analysis of the modified RNase

Aliquots (20 μL) of the post-dialysis RNase solutions were placed on microscopic slides, covered with microscopic cover glass (22 mm in diameter), and sealed. Micrographic images were captured with a SIM (SIMultaneous) Scanner on an Olympus Fluoview 1000 laser scanning confocal microscope (Olympus Bx61 microscope with a 10× dry objective lens) and analyzed using Olympus Fluoview acquisition software. Scale bar representations are specified under the figure caption. The reference control micrograph was obtained using a solution containing the unmodified RNase (0.050 mM).

2.5. Detection of biomineralization by scanning electron microscopy (SEM)

Aliquots (5 μL) of the unmodified RNase and the post-dialysis RNase solutions were deposited on a microscopic cover glass (22 mm in diameter) and fixed with an equal volume of the SEM matrix made of 4% formaldehyde in phosphate-buffered saline (PBS) containing [NaCl] = 137 mM, [KCl] = 2.7 mM, [Na_2HPO_4] = 10 mM, [KH_2PO_4] = 2 mM, followed by air-drying for 2 h at room temperature. Then, the samples were dehydrated in ethanol in ascending percentage concentrations (30%, 50%, 70%, 80%, 90%, 100%) for 20 min each. For a control sample, an aliquot of the SEM matrix was mixed with an equal volume of milliQ water, and the residue was submitted to the same dehydration procedure described above. Scanning electron micrographs were collected using a JEOL Neoscope microscope operating with an accelerating voltage of 10 kV.

3. Results

3.1. RNase modification detected by SDS–PAGE

SDS–PAGE analysis was carried out after RNase was incubated with pBQ in a concentration- and time-dependent manner. The incubation reactions were carried out by reacting RNase with pBQ at two different concentrations (0.50 and 5.0 mM), at various time periods, in phosphate buffer (pH 7.0, 50 mM) at 37 °C. Fig. 2 illustrates the gel features of the pBQ-treated RNase, where pBQ concentrations were 0.50 and 5.0 mM, respectively, and incubation time periods were every 10 min from 10 to 50 min and every 60 min from 60 to 300 min.

When RNase was treated with 0.50 mM pBQ, a protein band with the determined MW of 33 kDa appeared in addition to the control band at the bottom of the gel (Fig. 2A), and this occurred as early as 10 min of incubation. After 120 min, a second band, however dimmer, appeared at 53 kDa region and the intensity of the second band increased as the incubation time increased up to 300 min (Fig. 2B). A third band appeared very faintly at 70 kDa region when RNase was incubated for more than 180 min. As pBQ concentration increased to 5.0 mM (Fig. 2C/D), the extent of RNase modification intensified. With 5.0 mM of pBQ, multiple protein bands appeared as early as 10 min at the regions of 33, 53, and 70 kDa. In addition to the multiple bands appearing at the region lower than the 84 kDa marker, a smearing band showed up at the higher MW region as the incubation time increased to 30 min or longer. The SDS–PAGE experiment for control RNase shows no change up to 24-h incubation at 37 °C (see Supplementary data).

3.2. Fluorescence spectroscopy and anisotropy determination

In addition to SDS–PAGE experiments, to furthermore examine RNase modifications induced by pBQ, the fluorescence behavior of RNase (0.050 mM) as well as RNase (0.050 mM) treated with pBQ at various concentrations (0.050, 0.25, 0.50, and 1.50 mM) in phosphate buffer (pH 7.0, 50 mM) was monitored for 24 h at 37 °C. The fluorescence spectrum of the unmodified RNase, as well as those of the modified RNase, shows a band centered around 300 nm. In the reaction mixture, this band partially overlaps with the fluorescence band of hydroquinone (HQ, the product of pBQ reduction) centered around 330 nm. Although HQ concentration is very low at the beginning of the reaction, particularly for the reactions with lower pBQ concentrations, and its interference is small, HQ concentration increases in time and the fluorescence spectra of the reaction mixtures become dominated by it, especially for higher pBQ concentrations. To minimize this interference while maintaining measurable fluorescence intensity, the monitoring of the changes in the RNase fluorescence intensity was performed at 295 nm and at 300 nm. In addition, fluorescence anisotropy values were also determined and monitored for 24 h at the same wavelengths.

Fig. 3 shows the changes in the fluorescence intensity at the observed wavelengths as the protein modification occurred over 24 h as well as the changes observed in the anisotropy. The fastest and the most significant decrease in the fluorescence intensity occurred for the reaction mixture with the ratio of pBQ:RNase = 30:1. The decrease in the fluorescence intensity is so dramatic that the anisotropy determination became unreliable after 4 h due to extremely low intensity. Fig. 3 also shows that anisotropy values, at both investigated wavelengths, tend to decrease as the reaction progresses. It is found however that the anisotropy values for the modified RNase, obtained after removal of pBQ and HQ through dialysis, are larger than those of the reaction mixture at 24 h, and even slightly larger than these values of the unmodified RNase. Table 1 lists the anisotropy values for the unmodified RNase and the modified RNase.

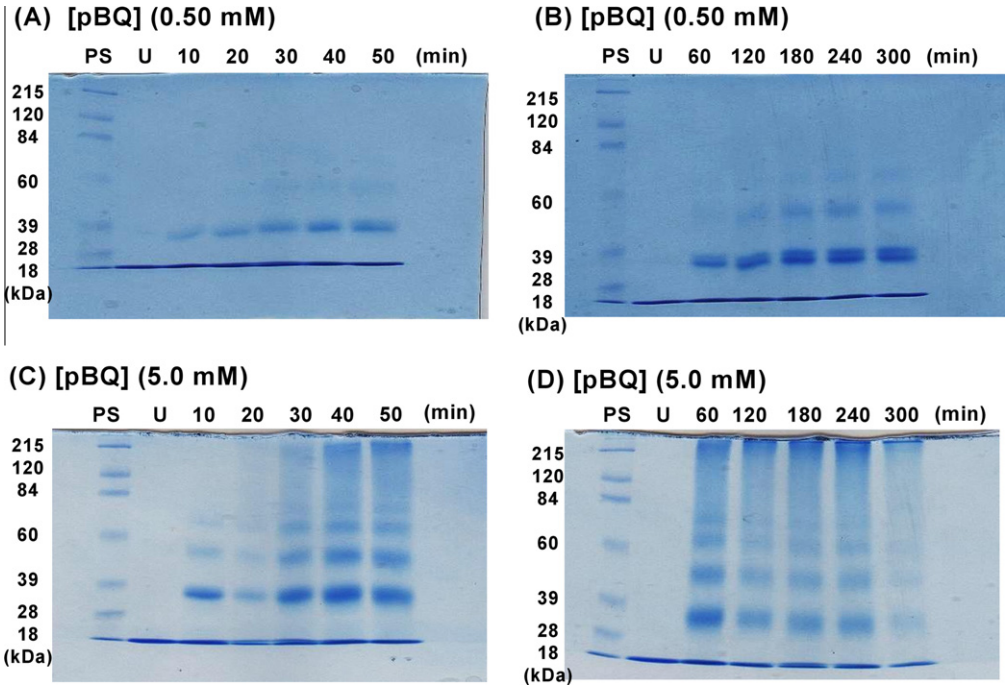

Fig. 2. Concentration- and time-dependent modification of RNase upon exposure to pBQ at 0.50 and 5.0 mM. All reactions were carried out in phosphate buffer (pH 7.0, 50 mM) at 37 °C. PS, protein standard molecular marker; U, unmodified control RNase. (A) RNase was incubated with 0.50 mM pBQ for 10, 20, 30, 40, 50 min. (B) RNase was incubated with 0.50 mM pBQ for 60, 120, 180, 240, 300 min. (C) RNase was incubated with 5.0 mM pBQ for 10, 20, 30, 40, 50 min. (D) RNase was incubated with 5.0 mM pBQ for 60, 120, 180, 240, 300 min.

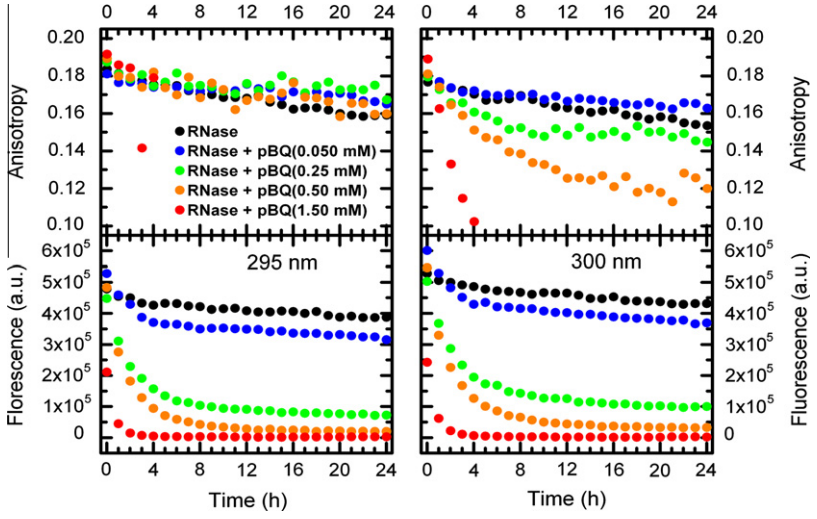

Fig. 3. Fluorescence intensity and anisotropy at 295 and 300 nm for RNase (0.050 mM) and reaction mixtures containing RNase (0.050 mM) and pBQ (0.050, 0.25, 0.50, 1.50 mM) at 37 °C.

The fluorescence spectra of the unmodified and the modified (*i.e.*, post-dialysis) RNase are shown in Fig. 4A. The fluorescence intensity of the modified RNase is lower than that of the unmodified RNase, and the intensity decreases as pBQ concentration increases. The normalized integrated fluorescence intensity in the 290–360 nm range vs. the pBQ concentration is given in the inset of Fig. 4A.

3.3. UV–Vis spectroscopic analysis

Fig. 4B shows the representative UV–Vis spectra of the post-dialysis RNase obtained after RNase was treated with pBQ at various concentrations (0.050, 0.25, 0.50, and 1.50 mM) at 37 °C and

Table 1
Anisotropy values for RNase and modified[a] RNase at 37 °C.

	295 nm	300 nm
RNase	0.169	0.166
RNase modified by pBQ (0.050 mM)	0.173	0.173
RNase modified by pBQ (0.25 mM)	0.186	0.181
RNase modified by pBQ (0.50 mM)	0.185	0.188
RNase modified by pBQ (1.50 mM)[b]	0.23	0.21

[a] After dialysis.
[b] Due to the low fluorescence intensity of this solution, these determined values should be considered just rough estimates.

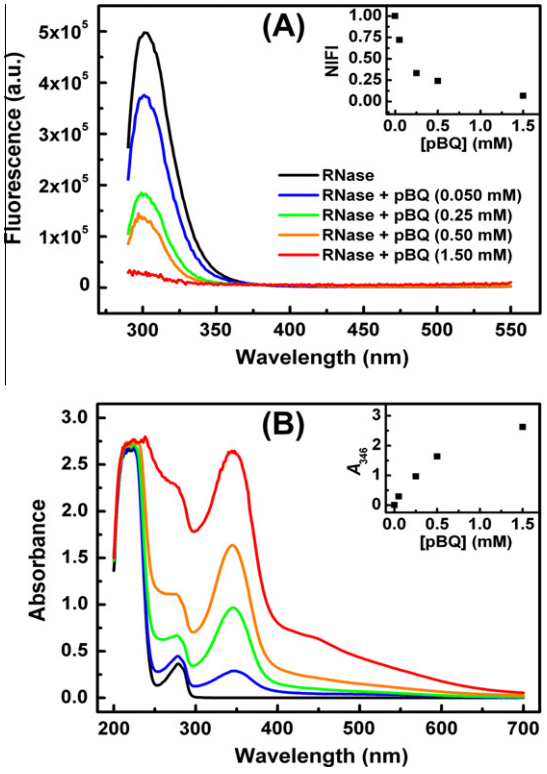

Fig. 4. (A) Fluorescence and (B) UV–Vis spectra of RNase (0.050 mM) and the post-dialysis RNase modified by pBQ (0.050, 0.25, 0.50, 1.50 mM) for 24 h at 37 °C. Inset panel A: Normalized integrated fluorescence intensity (NIFI) in the 290–360 nm range vs. pBQ concentration. Inset panel B: Plot of absorbance at 346 nm of the modified RNase vs. pBQ concentration.

pH = 7.0 for 24 h. As shown in Fig. 4B, the control sample containing the unmodified RNase (0.050 mM) has the maximum absorption at 280 nm. Unlike the control RNase, an additional chromophore developed at 346 nm in the modified RNase as pBQ reacted with RNase. This additional chromophore is consistent with the visually observed red-brown color of the modified RNase solution. As pBQ concentration increased from 0.050 mM to 1.50 mM, A_{346} increased, however not in a linear manner, and the increase of A_{346} slowed down at the higher concentration of pBQ.

3.4. Confocal microscopic analysis

In order to monitor morphological changes in the modified RNase, confocal microscopic measurements were carried out. Fig. 5 represents the micrographs for the series of dialyzed reactions when RNase was treated with pBQ at various concentrations (0.050, 0.25, 0.50, and 1.50 mM) at 37 °C and pH = 7.0 for 24 h. As samples were visualized, the focal plane was not deep enough to capturing all unmodified RNase moieties in one micrograph. As RNase was treated with higher pBQ concentrations, the shape and the size of RNase changed slightly and the micrographic image improved. As shown in Fig. 5A, the micrograph for the unmodified RNase illustrates proteins of a relatively uniform shape and small size. As pBQ concentration increased to 0.50 mM (pBQ:RNase = 10:1), there were noticeable changes as protein aggregates appeared in various sizes with a decrease in the number of protein structures with smaller sizes and an increase in the number of larger aggregates. As pBQ concentration increased to 1.50 mM (pBQ:RNase = 30:1), the nature of the modification became obvious with only the larger protein aggregates observed.

3.5. SEM microscopic analysis

In recent years, the interaction between proteins and salts has been an interest to biochemists and material scientists. In an effort to shed light on the role of the modified RNase on mineralization of commonly found salts in biological systems, we observed SEM morphology of crystallized salts with or without the presence of RNase whether modified with pBQ or not. For a control, we prepared a sample by taking an aliquot of the SEM matrix made of PBS and 4% formaldehyde. The SEM matrix is ideal for the study, since it consists of PBS containing commonly found ions in biological systems such as sodium, potassium, and phosphate ions [45]. In addition, both the unmodified and the modified RNase were treated with the same SEM matrix as well, in order to monitor the effect of the presence of RNase. The control sample shows the salt crystals with the length of 1 mm approximately (Fig. 6A). All salt crystals of the SEM matrix alone have a pyramidal structure in a similar manner. The micrograph of the SEM matrix in the presence of the unmodified RNase shows that the length of the salt crystals decreased to 500 μm or shorter (Fig. 6B). Furthermore, the SEM image containing the modified RNase in the SEM matrix reveals that not only the size of the salt crystals appears to vary but also the shape of the crystals is very polymorphic. This trend is consistently observed for all SEM samples containing the modified RNase treated with various concentrations of pBQ.

4. Discussion

As mentioned above, PAH quinones such as pBQ are thought to exhibit their toxicity mainly through redox cycling and adduct formation. We also postulated the possibility of pBQ-induced protein cross-linking leading to protein aggregation. In the present study, we found evidence that pBQ induces RNase modifications through both adduct formation and protein aggregation.

Our SDS–PAGE results show that pBQ induces oligomerization of RNase, based on the observed protein bands at 33, 53, and 70 kDa, and polymeric aggregation observed as the smearing band in the higher MW region. Based on MW of RNase (13.7 kDa), the estimated MW of RNase oligomers such as dimers, trimers, and tetramers are 27, 41, and 55, respectively. These values are calculated without considering the contribution from the covalently linked

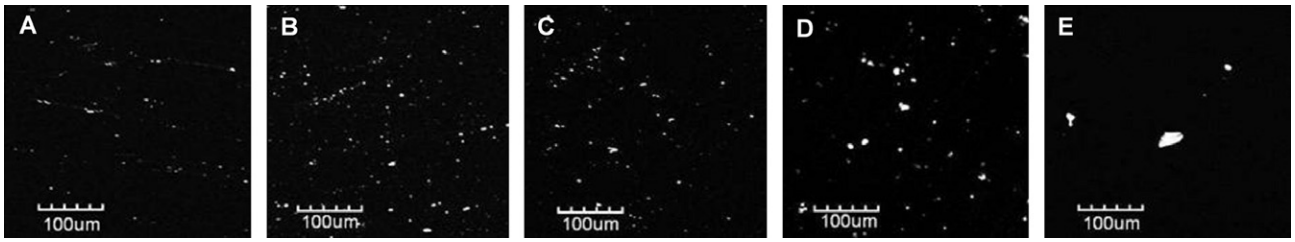

Fig. 5. Confocal micrographs of the unmodified RNase (0.050 mM) and the post-dialysis RNase modified by pBQ for 24 h at 37 °C. (A) Unmodified RNase. (B) RNase modified by pBQ (0.050 mM). (C) RNase modified by pBQ (0.25 mM). (D) RNase modified by pBQ (0.50 mM). (E) RNase modified by pBQ (1.50 mM). Scale bar represents 100 μm.

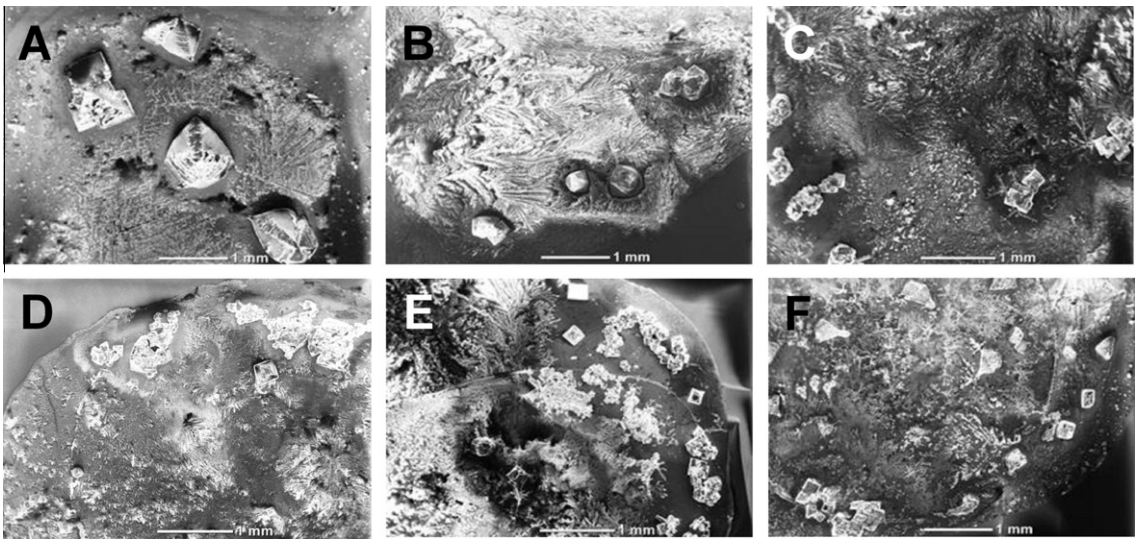

Fig. 6. SEM micrographs of SEM matrix ± RNase. (A) SEM matrix. (B) SEM matrix + unmodified RNase. (C) SEM matrix + RNase modified by pBQ (0.050 mM). (D) SEM matrix + RNase modified by pBQ (0.25 mM). (E) SEM matrix + RNase modified by pBQ (0.50 mM). (F) SEM matrix + RNase modified by pBQ (1.50 mM). Scale bar represents 1 mm.

pBQ to the total MW of the modified RNase. The observed higher MW values of the modified RNase than the expected MW values for the RNase oligomers indicates some degree of alkylation of amino acid residues by pBQ. This adduct formation occurs simultaneously with RNase going through cross-linking to form oligomers. These results indicate that pBQ is very efficient in modifying RNase leading to not only adduct formation but also severe protein aggregation. Also, it should be noted that, based on the time-dependent incubation experiments, the pBQ-induced oligomerization occurred prior to the polymeric aggregation. Therefore, we believe that pBQ governs the RNase aggregation in a stepwise process involving RNase oligomerization in initial steps followed by RNase polymerization in subsequent steps.

The adduct formation of pBQ and RNase is also consistent with the UV–Vis spectra of the modified RNase and the increasing absorbance at 346 nm. Since the spectra were obtained after dialysis, unbound pBQ and HQ were removed at this point. Therefore, the species absorbing at 346 nm are believed to be pBQ covalently linked to amino acid residues. This band is present even for the pBQ:RNase = 1:1 reaction condition, which is expected to produce predominantly adduct formation without leading to extensive protein aggregation. The observed plateauing in the A_{346} increase, associated with a saturation in the adduct formation, is expected since this is limited by the number of amino acid residues in RNase that can form covalent bonds with pBQ. RNase has several nucleophilic amino acids in its sequence, including 10 lysines, 15 serines, 8 cysteines, and 6 tyrosines [46]. Previously, Hanzlik and coworkers identified the (2,5-quinonyl)-*S*-protein adduct formed between pBQ and a cysteine residue of RNase [16], which was found to be susceptible for further alkylation by other amino acids like lysine by Lau and coworkers [17,18,20,21]. In addition, recent work by Lau and coworkers indicates that pBQ is able to alkylate amino acids such as lysine and glutamic acid in a complex manner, however using cytochrome c as a model protein [18–21]. In accordance with the previously reported studies, our combined SDS–PAGE and UV–Vis results show that pBQ can efficiently alkylate amino acid residues in RNase as well.

The formation of polymeric aggregates was further monitored by confocal microscopy. As presented in Fig. 5, as the incubation concentration of pBQ increased from 0.050 mM to 1.50 mM, confocal images show that the size of the proteins increased. This finding strongly suggests that the presence of pBQ resulted in severe RNase polymerization, especially at the higher concentration of pBQ. However, it should be noted that 30 equivalents of pBQ (*i.e.*, 1.50 mM) was utilized to monitor RNase modification under drastic condition, and this concentration is not physiologically viable. Overall, the confocal microscopic analysis visually confirms that RNase underwent cross-linking induced by pBQ leading to extensive protein aggregation.

The higher anisotropy values determined at 295 and 300 nm for the modified RNase compared with those of the unmodified RNase (Table 1) are associated with a larger rotational correlation time and, assuming similar lifetimes, with a larger molecular volume [47] for the modified RNase. This finding is also consistent with an increase in the MW of the modified RNase through adduct formation and aggregation.

The anisotropy of the reaction mixture shows a steady decline both at 295 nm and at 300 nm during the 24 h monitoring of the reaction (Fig. 3). This anisotropy reduction is more significant at 300 nm and this is, at least in part, due to some interference from the low anisotropy of HQ, whose concentration is also building up as time progresses. The decreasing anisotropy trend suggests that it is possible that RNase undergoes some conformational changes in time, producing species with lower anisotropy. These changes of RNase are probably reversible because the post-dialysis RNase samples (Table 1) exhibited slightly higher anisotropy values than those of the 24-h incubated, pre-dialysis samples (Fig. 3).

Based on the normalized integrated fluorescence intensity (NIFI) of the unmodified and the modified RNase (inset of Fig. 4A), one can estimate a degree of protein modification (DPM) defined as DPM = 1 − NIFI. DPM is expected to be larger for a higher concentration of pBQ in the reaction mixture and smaller for a lower concentration of pBQ. Indeed, DPM based on integrated fluorescence intensity in the 290–360 nm range is estimated to be 0.28, 0.67, 0.76, and 0.93 for pBQ concentrations of 0.050, 0.25, 0.50, and 1.50 mM, respectively. Considering that the RNase fluorescence is primarily due to six tyrosine residues, the calculated DPM values suggest the quenching of fluorescence from 2, 4, 5 and 6 tyrosine residues for pBQ concentrations of 0.050, 0.25, 0.50, and 1.50 mM, respectively. The low intensity fluorescence observed for the modified RNase by 1.50 mM pBQ and the fact that this modified RNase is mostly polymeric aggregates suggest that these aggregates exhibit very low fluorescence upon excitation at 280 nm.

SEM results suggest that electrolyte shielding influences the way salts crystallize in the presence of the unmodified or the modified RNase. Electrolyte shielding was previously observed and reported by Talapatra's [32] and Taboada's [35] groups. Their results indicate that electrolytes mitigate charge repulsion between proteins and increase the hydrophobic interaction between proteins leading to protein aggregation. We however sought to monitor the interaction between salts and modified proteins directly using SEM. Our SEM micrograph results show that the presence of the unmodified RNase altered salt crystallization slightly, while the modified RNase, with a more hydrophobic structure, altered salt crystallization more extensively leading to formation of polymorphic salt crystals in various lengths and shapes. This finding implies that the alteration of salt crystallization in the presence of RNase is due to salt-protein interaction mostly via electrolyte shielding, and that the nature of hydrophobicity of proteins plays a critical role in the interaction.

5. Conclusions

In this report, we present the results of an investigation on RNase modifications induced by pBQ, employing a variety of methods including SDS–PAGE, fluorescence spectroscopy, confocal microscopy, and scanning electron microscopy. This study shows that the biological role of pBQ in terms of RNase modification is rather complex leading to adduct formation, oligomerization, and polymeric aggregate formation. One of the most significant findings is the evidence of pBQ-induced RNase polymer aggregation using both SDS–PAGE and confocal microscopy. The degree of protein modification, estimated based on fluorescence intensity, was found to be in good agreement with the concentration of pBQ in the reaction mixture. The biomineralization of salts in the presence of the modified RNase was altered to a greater extend than in the presence of the unmodified RNase. Taken together, this study provides a better understanding of the nature of protein modifications induced by PAH metabolites.

Acknowledgments

The study was supported in part by UC Foundation Fund, Grote Fund, NSF-MRI Fund (DBI-922941), and Wheeler Research Fund. TVA work was supported by Tennessee Tech University through a Non-Instructional Faculty Assignment Grant. The research was conducted at the Department of Chemistry and the Department of Biological and Environmental Sciences at the University of Tennessee at Chattanooga.

Appendix A. Supplementary material

Supplementary data associated with this article can be found, in the online version, at doi:10.1016/j.bioorg.2011.11.002.

References

[1] J.E. Huff, J.K. Haseman, D.M. DeMarini, S. Eustis, R.R. Maronpot, A.C. Peters, R.L. Persing, C.E. Chrisp, A.C. Jacobs, Environ. Health Perspect. 82 (1989) 125–163.
[2] NTP toxicology and carcinogenesis studies of benzene (CAS No. 71-43-2) in F344/N rats and B6C3F1 mice (Gavage Studies), Natl. Toxicol. Program Tech. Rep. Ser. 289 (1986) 1–277.
[3] R. Snyder, C.C. Hedli, Environ. Health Perspect. 104 (6) (1996) 1165–1172.
[4] R. Snyder, E. Dimitriadis, R. Guy, P. Hu, K. Cooper, H. Bauer, G. Witz, B.D. Goldstein, Environ. Health Perspect. 82 (1989) 31–35.
[5] S. Kawanishi, Y. Hiraku, M. Murata, S. Oikawa, Free Radical Biol. Med. 32 (9) (2002) 822–832.
[6] S. Oikawa, K. Nishino, S. Oikawa, S. Inoue, T. Mizutani, S. Kawanishi, Biochem. Pharmacol. 56 (1998) 361–370.
[7] J.L. Bolton, M.A. Trush, T.M. Penning, G. Dryhurst, T.J. Monks, Chem. Res. Toxicol. 13 (3) (2000) 135–160.
[8] A. Chenna, B. Hang, B. Rydberg, E. Kim, K. Pongracz, W.J. Bodell, B. Singer, Proc. Natl. Acad. Sci. USA 92 (13) (1995) 5890–5894.
[9] A. Chenna, H. Maruenda, B. Singer, Synthesis of para-benzoquinone, IARC Sci. Publ. (150) (1999) 89–101.
[10] A. Chenna, B. Singer, Chem. Res. Toxicol. 8 (1995) 865–874.
[11] A. Chenna, B. Singer, Chem. Res. Toxicol. 10 (2) (1997) 165–171.
[12] K. Pongracz, W.J. Bodell, Chem. Res. Toxicol. 4 (2) (1991) 199–202.
[13] B. Hang, A. Chenna, H. Fraenkel-Conrat, B. Singer, Proc. Natl. Acad. Sci. USA 93 (24) (1996) 13737–13741.
[14] T.A. McDonald, S. Waidyanatha, S.M. Rappaport, Carcinogenesis 14 (9) (1993) 1921–1925.
[15] T.A. McDonald, K. Yeowell-O'Connell, S.M. Rappaport, Cancer Res. 54 (18) (1994) 4907–4914.
[16] R.P. Hanzlik, S.P. Harriman, M.M. Frauenhoff, Chem. Res. Toxicol. 7 (2) (1994) 177–184.
[17] W. Yue, Y.M. Koen, T.D. Williams, R.P. Hanzlik, Chem. Res. Toxicol. 18 (11) (2005) 1748–1754.
[18] A.A. Fisher, M.T. Labenski, S. Malladi, V. Gokhale, M.E. Bowen, R.S. Milleron, S.B. Bratton, T.J. Monks, S.S. Lau, Biochemistry 46 (39) (2007) 11090–11100.
[19] A.A. Fisher, M.T. Labenski, S. Malladi, J.D. Chapman, S.B. Bratton, T.J. Monks, S.S. Lau, Toxicol. Sci. 122 (1) (2011) 64–72.
[20] M.D. Person, D.E. Mason, D.C. Liebler, T.J. Monks, S.S. Lau, Chem. Res. Toxicol. 18 (1) (2005) 41–50.
[21] M.D. Person, T.J. Monks, S.S. Lau, Chem. Res. Toxicol. 16 (5) (2003) 598–608.
[22] W. Zaborska, B. Krajewska, M. Kot, W. Karcz, Bioorg. Chem. 35 (3) (2007) 233–242.
[23] J.M. Berg, J.L. Tymoczko, L. Stryer, Biochemistry, sixth ed., W.H. Freeman and Co., New York, 2006.
[24] F. Bemporad, G. Calloni, S. Campioni, G. Plakoutsi, N. Taddei, F. Chiti, Acc. Chem. Res. 39 (9) (2006) 620–627.
[25] F. Chiti, C.M. Dobson, Annu. Rev. Biochem. 75 (2006) 333–366.
[26] F. Chiti, C.M. Dobson, Nat. Chem. Biol. 5 (1) (2009) 15–22.
[27] C.M. Dobson, Nature 426 (6968) (2003) 884–890.
[28] M. Ramirez-Alvarado, Prog. Mol. Biol. Transl. Sci. 84 (2008) 115–160.
[29] N. Gregersen, P. Bross, S. Vang, J.H. Christensen, Annu. Rev. Genom. Human Genet. 7 (2006) 103–124.
[30] T. Yang, Y. Zhang, Z. Li, Biomacromolecules 12 (6) (2011) 2027–2031.
[31] M. Dumoulin, J.R. Kumita, C.M. Dobson, Acc. Chem. Res. 39 (9) (2006) 603–610.
[32] P. Pal, M. Mahato, T. Kamilya, B. Tah, R. Sarkar, G.B. Talapatra, J. Phys. Chem. B 115 (14) (2011) 4259–4265.
[33] T. Borwankar, C. Rothlein, G. Zhang, A. Techen, C. Dosche, Z. Ignatova, Biochemistry 50 (12) (2011) 2048–2060.
[34] N.K. Pandey, S. Ghosh, S. Dasgupta, J. Phys. Chem. B 114 (31) (2011) 10228–10233.
[35] J. Juarez, S.G. Lopez, A. Cambon, P. Taboada, V. Mosquera, J. Phys. Chem. B 113 (30) (2009) 10521–10529.
[36] G. Calloni, C. Lendel, S. Campioni, S. Giannini, A. Gliozzi, A. Relini, M. Vendruscolo, C.M. Dobson, X. Salvatella, F. Chiti, J. Am. Chem. Soc. 130 (39) (2008) 13040–13050.
[37] T.N. Niraula, T. Konno, H. Li, H. Yamada, K. Akasaka, H. Tachibana, Proc. Natl. Acad. Sci. USA 101 (12) (2004) 4089–4093.
[38] T.N. Niraula, K. Haraoka, Y. Ando, H. Li, H. Yamada, K. Akasaka, J. Mol. Biol. 320 (2) (2002) 333–342.
[39] M. Zhu, D.C. Spink, B. Yan, S. Bank, A.P. DeCaprio, Chem. Res. Toxicol. 8 (5) (1995) 764–771.
[40] D. Lin, H.-g. Lee, Q. Liu, G. Perry, M.A. Smith, L.M. Sayre, Chem. Res. Toxicol. 18 (2005) 1219–1231.
[41] C. Alt, P. Eyer, Chem. Res. Toxicol. 11 (10) (1998) 1223–1233.
[42] V. Pipich, M. Balz, S.E. Wolf, W. Tremel, D. Schwahn, J. Am. Chem. Soc. 130 (21) (2008) 6879–6892.
[43] U.K. Laemmli, Nature 227 (5259) (1970) 680–685.
[44] K. Weber, M. Osborn, J. Biol. Chem. 244 (1969) 4406–4412.
[45] J. Sambrook, D.W. Russell, Molecular Cloning: A Laboratory Manual, vol. 3, Cold Spring Harbor Laboratory Press, Cold Spring Harbor, NY, 2001.
[46] D.G. Smyth, W.H. Stein, S. Moore, J. Biol. Chem. 238 (1963) 227–234.
[47] J.R. Lakowicz, Principles of Fluorescence Spectroscopy, third ed., Springer, New York, NY, 2006.